A near-infrared and lysosome-targeted BODIPY photosensitizer for photodynamic and photothermal synergistic therapy

Yan Liu[abc], Jie Gao[abc], Hongyu Li[abc], Mingyan Yang[abc], Yaping Zhou[ab], Zeli Yuan[abc]*, Xinmin Li [abc]*

[a]College of Pharmacy, Zunyi Medical University, Zunyi, Guizhou 563003, China;
[b]Key Laboratory of Basic Pharmacology of Ministry of Education and Joint International Research Laboratory of Ethnomedicine of Ministry of Education, Zunyi Medical University, Zunyi, Guizhou 563000, China;
[c]Guizhou International Scientific and Technological Cooperation Base for Medical Photo-Theranostics Technology and Innovative Drug Development, Zunyi, Guizhou 563003, China.

Table of Contents

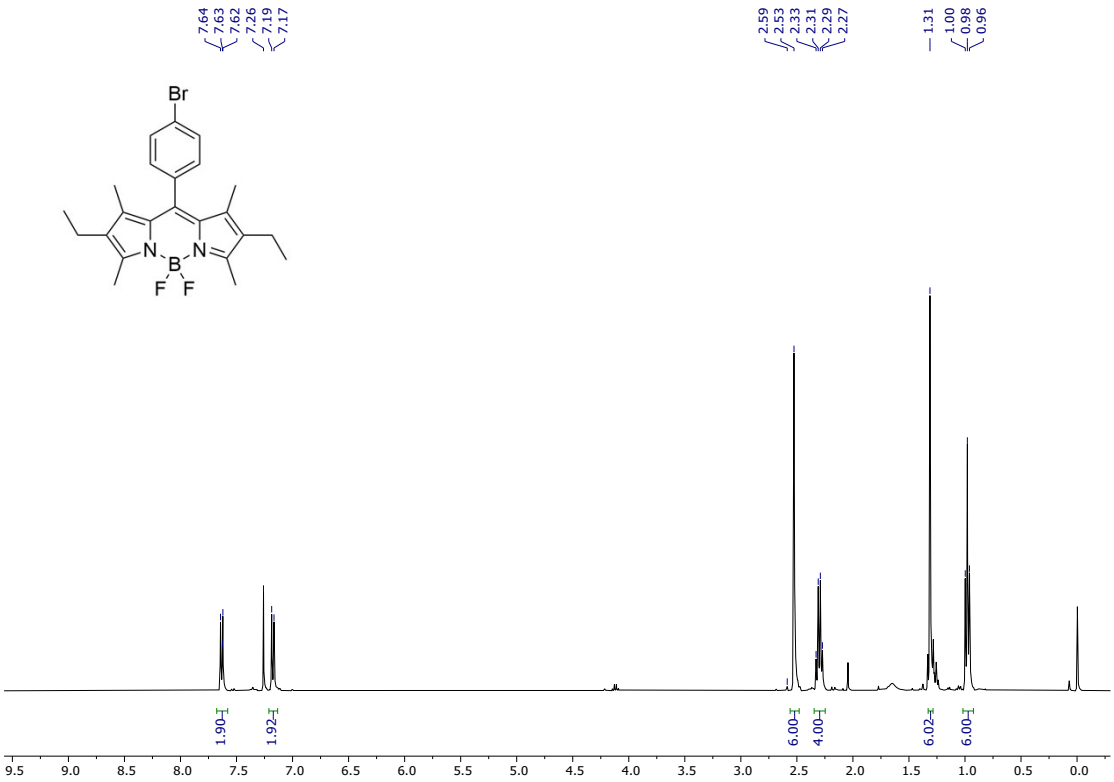

Fig. S1.[1]H NMR spectrum of BDP in $CDCl_3$.

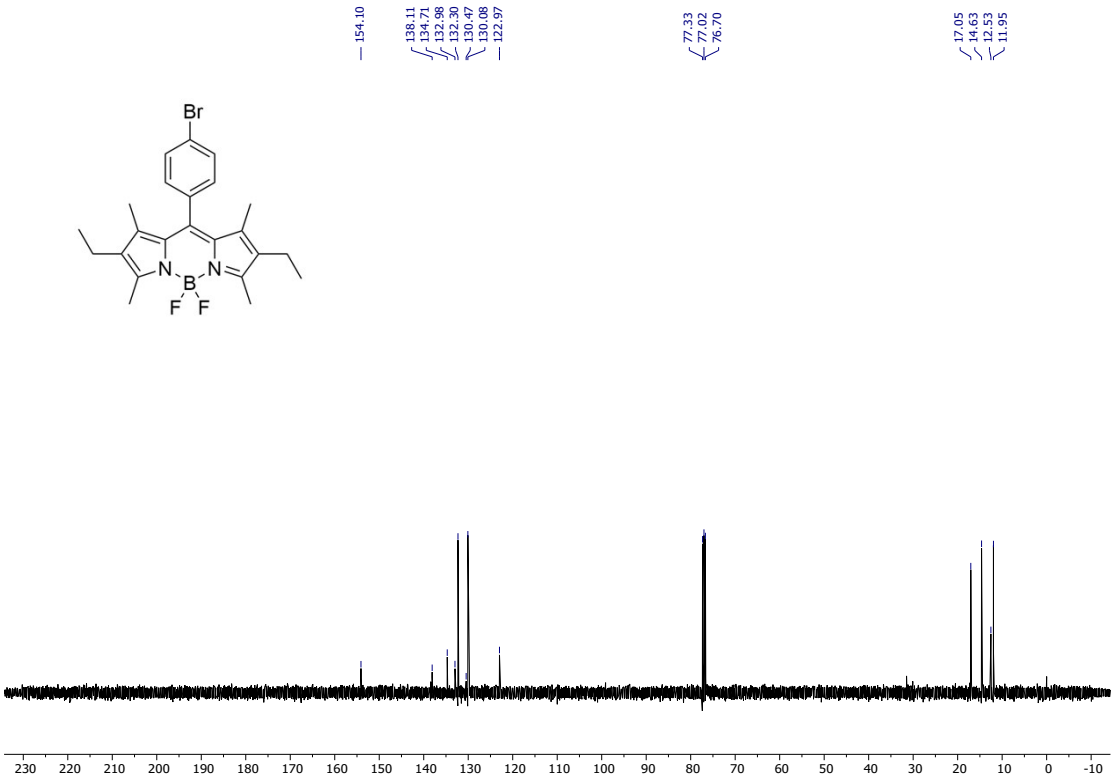

Fig. S2.[13]C NMR spectrum of BDP in $CDCl_3$.

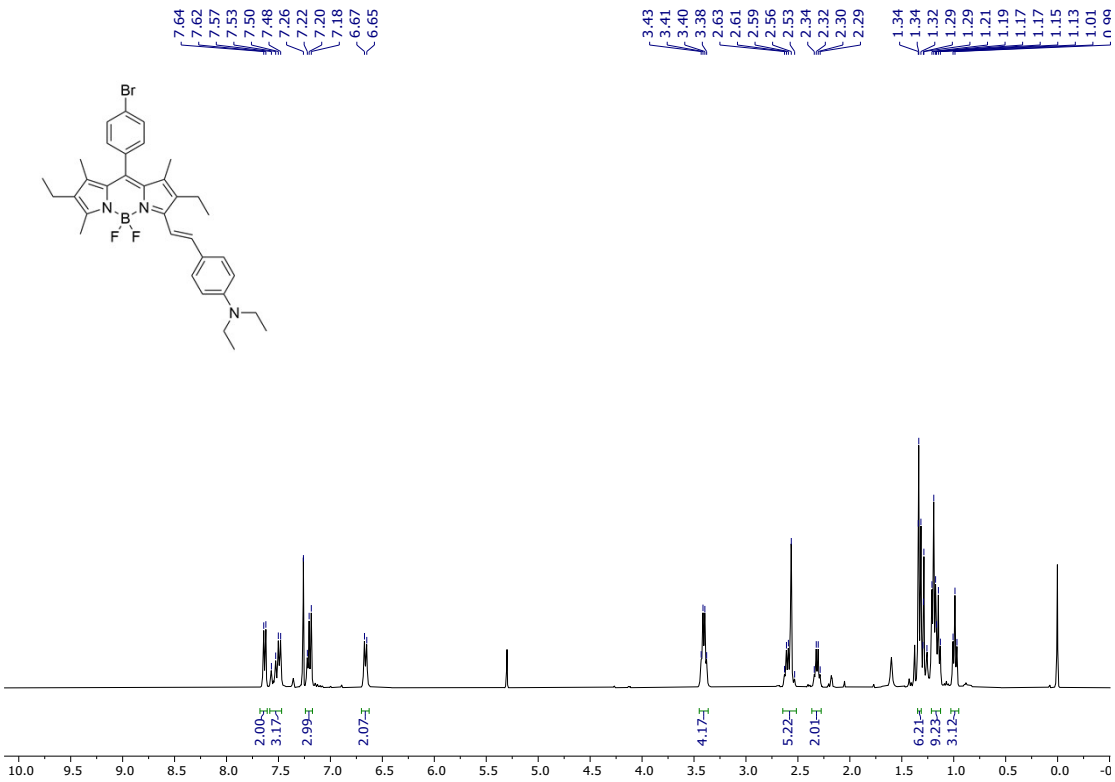

Fig. S3.[1]H NMR spectrum of Br-BDP in $CDCl_3$.

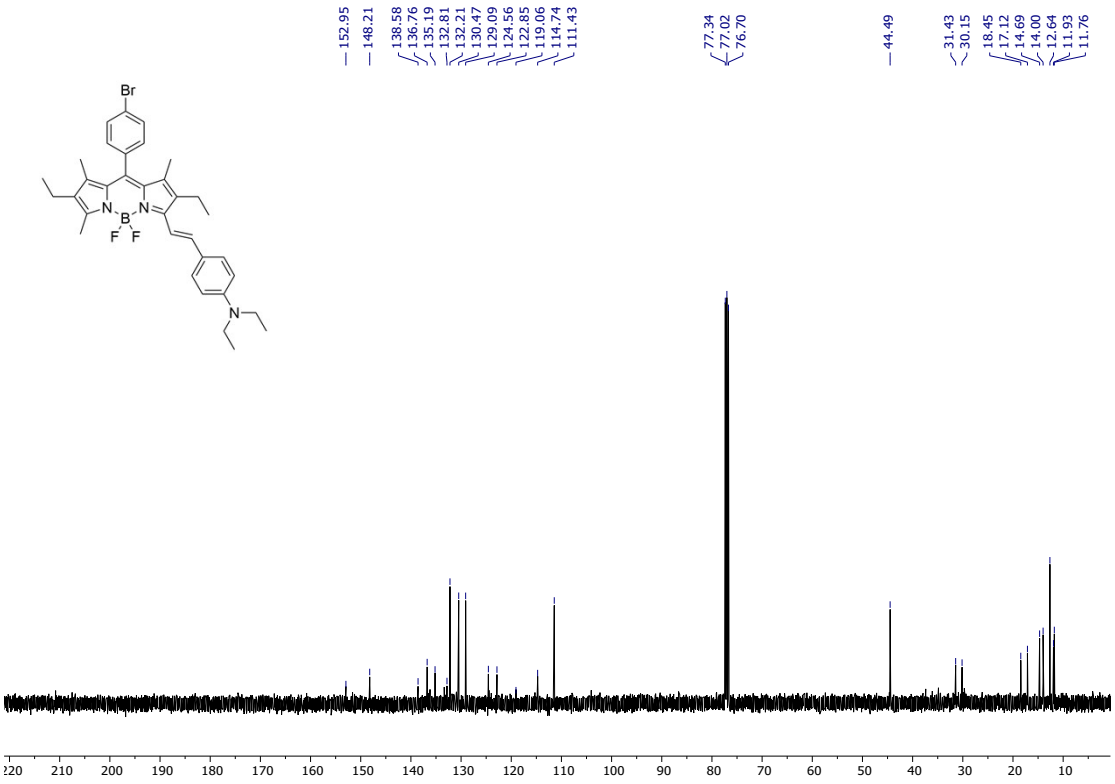

Fig. S4.[13]C NMR spectrum of Br-BDP in $CDCl_3$.

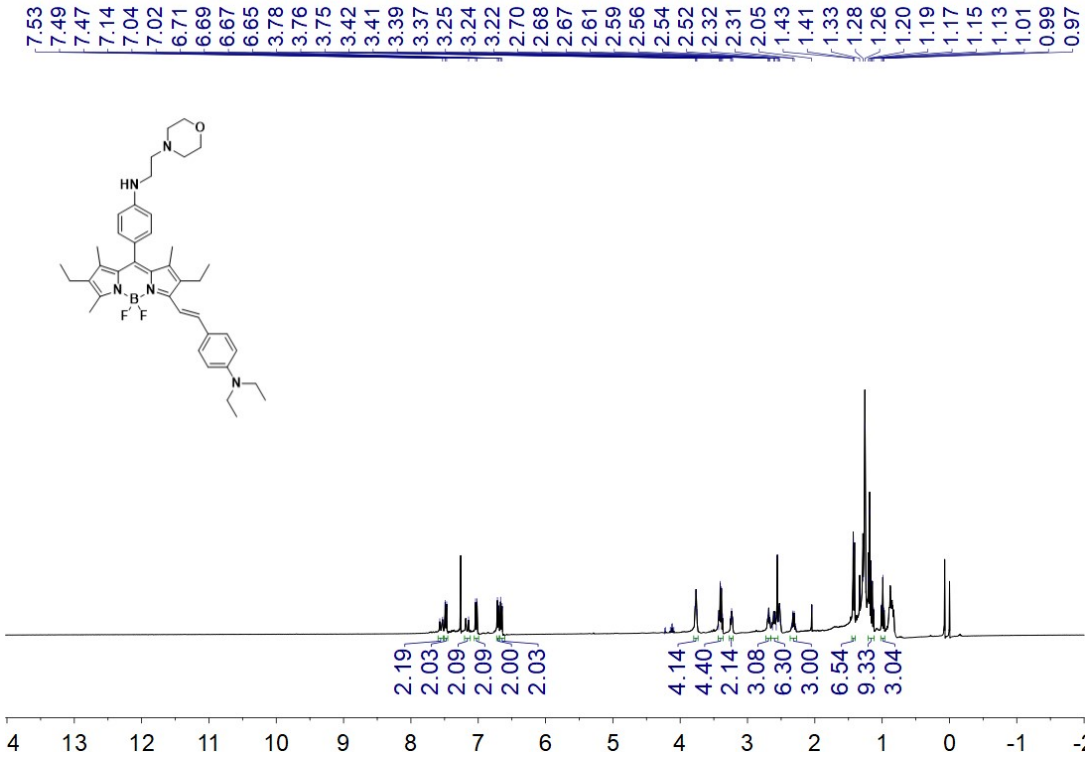

Fig. S5.[1]H NMR spectrum of Lyso-BDP in $CDCl_3$.

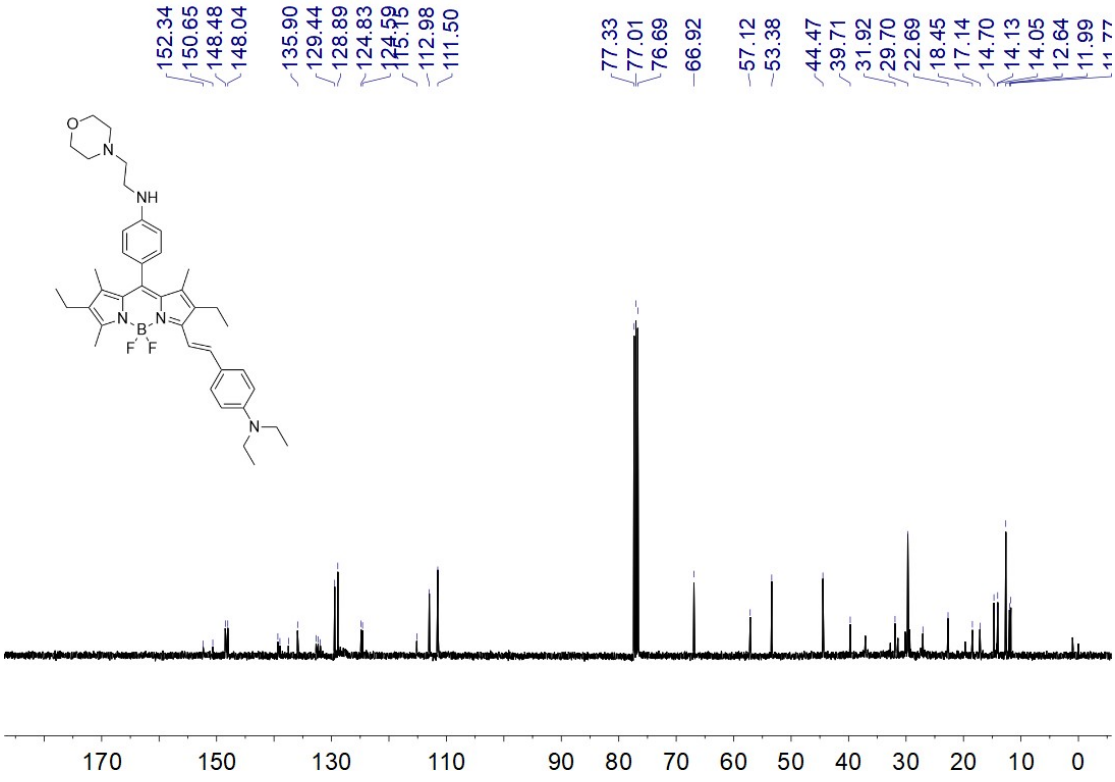

Fig. S6.[13]C NMR spectrum of Lyso-BDP in $CDCl_3$.

Compound Table

Compound Label	RT	Mass	Abund	Formula	Tgt Mass	Diff (ppm)
Cpd 1: C23 H26 B Br F2 N2	0.162	457.1397	130035	C23 H26 B Br F2 N2	457.1377	4.35

MS Zoomed Spectrum

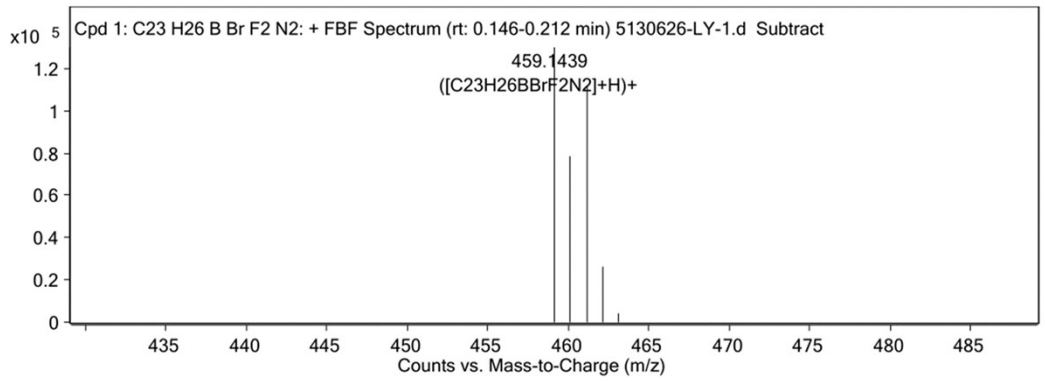

Fig. S7. High resolution mass spectrometry of BDP.

Compound Table

Compound Label	RT	Mass	Abund	Formula	Tgt Mass	Diff (ppm)
Cpd 1: C34 H39 B Br F2 N3	1.446	616.2441	1795061	C34 H39 B Br F2 N3	616.2425	2.43

MS Zoomed Spectrum

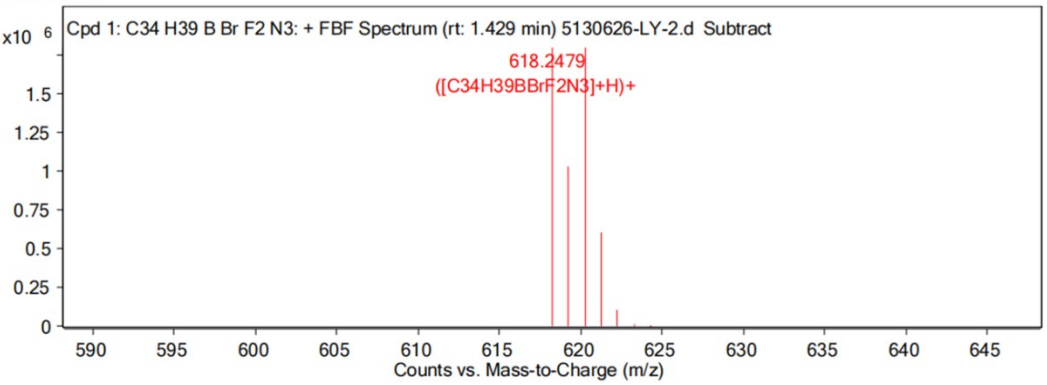

Fig. S8. High resolution mass spectrometry of Br-BDP.

Compound Table

Compound Label	RT	Mass	Abund	Formula	Tgt Mass	Diff (ppm)
Cpd 1: C40 H52 B F2 N5 O	0.171	666.4287	2249113	C40 H52 B F2 N5 O	666.4269	2.58

MS Zoomed Spectrum

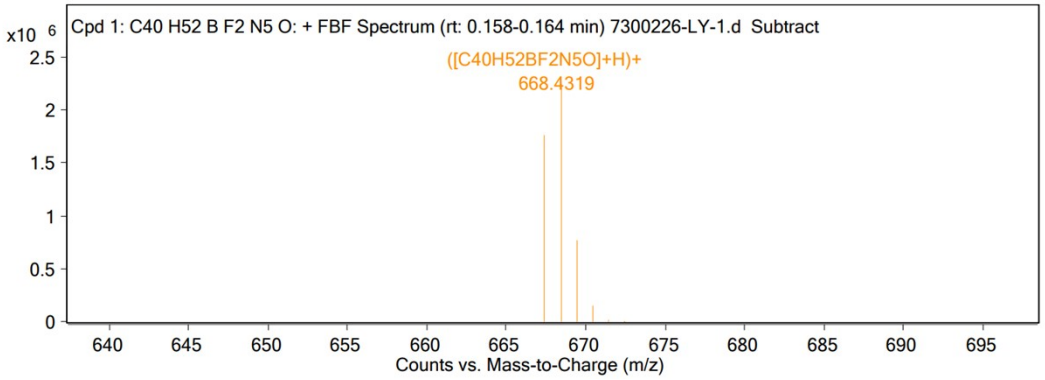

Fig. S9. High resolution mass spectrometry of Lyso-BDP.

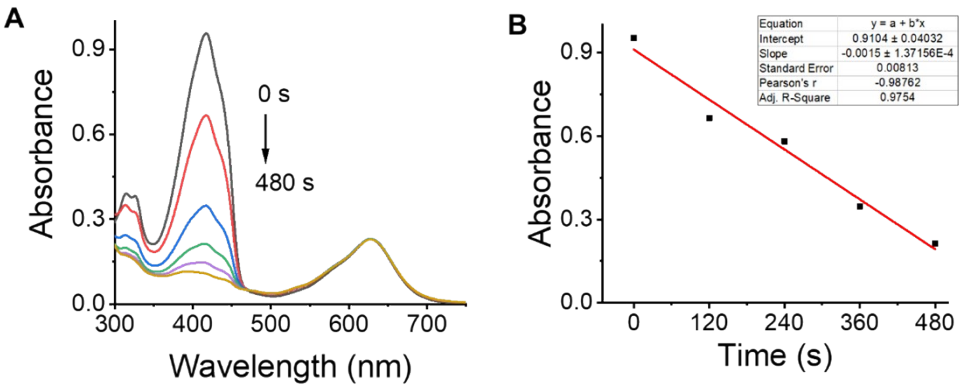

Fig. S10. (A) Change in the absorbance spectrum of the trap molecule DPBF seen in the presence of Lyso-BDP. (B) Lyso-BDP in DMSO as a function of irradiation (660 nm,0.2 W/cm^2) time.

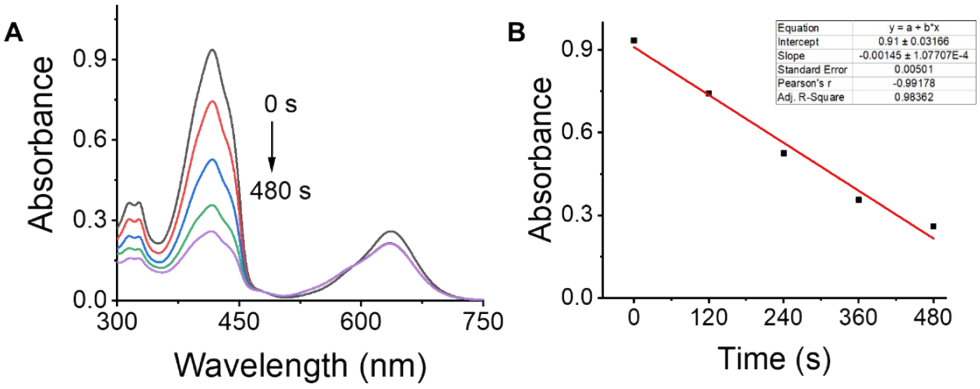

Fig. S11. (A) Change in the absorbance spectrum of the trap molecule DPBF seen in the presence of Br-BDP. (B) Br-BDPin DMSO as a function of irradiation (660 nm,0.2 W/cm^2) time.

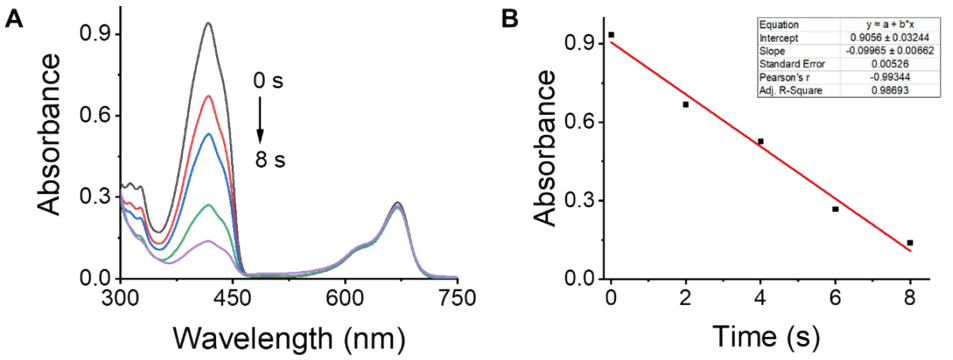

Fig. S12. (A) Change in the absorbance spectrum of the trap molecule DPBF seen in the presence of MB (0.52 in DMSO)[1]. (B) MB in DMSO as a function of irradiation (660 nm,0.2 W/cm^2) time.

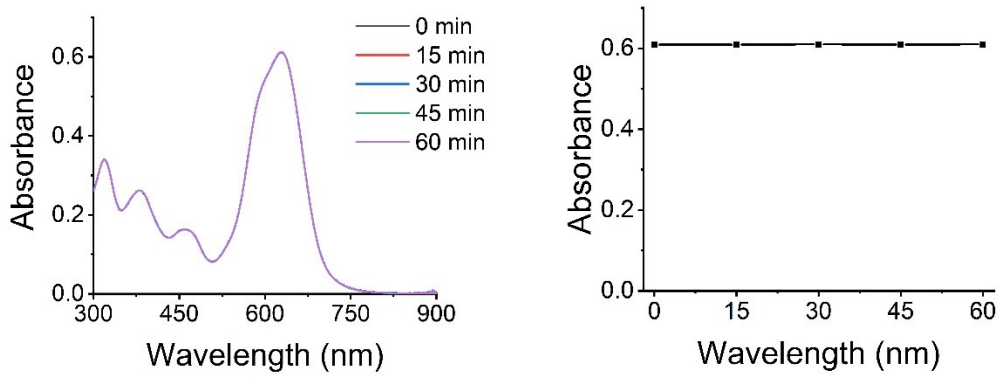

Fig. S13. The absorbance of **Lyso-BDP** under laser irradiation (660 nm, 0.2 W/cm^2) at different time.

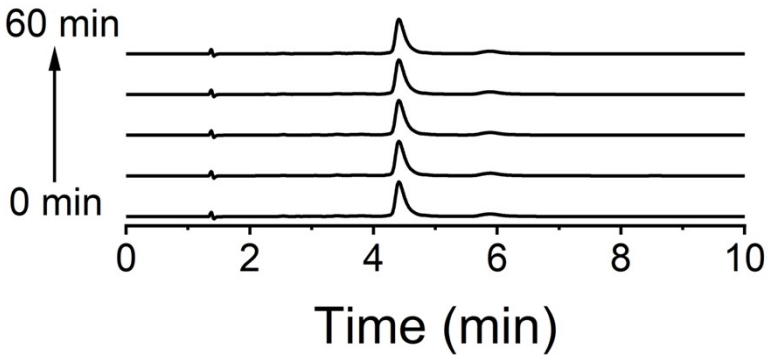

Fig. S14. The HPLC analysis of Lyso-BDP under different laser irradiation time (660 nm, 0.2 W/cm2), t_R = 4.4 min.

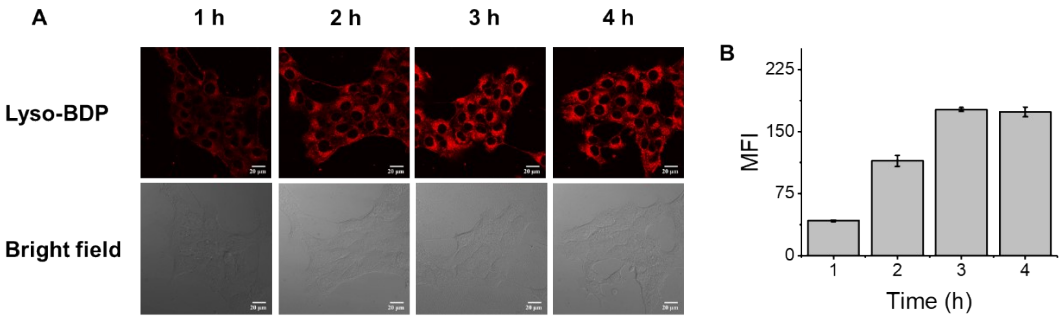

Fig. S15. (A) Fluorescence imaging of uptake of Lyso-BDP (10 μM) by 4T1 cells at different incubation times and (B) mean fluorescence intensity. Scale bar, 20 μm.

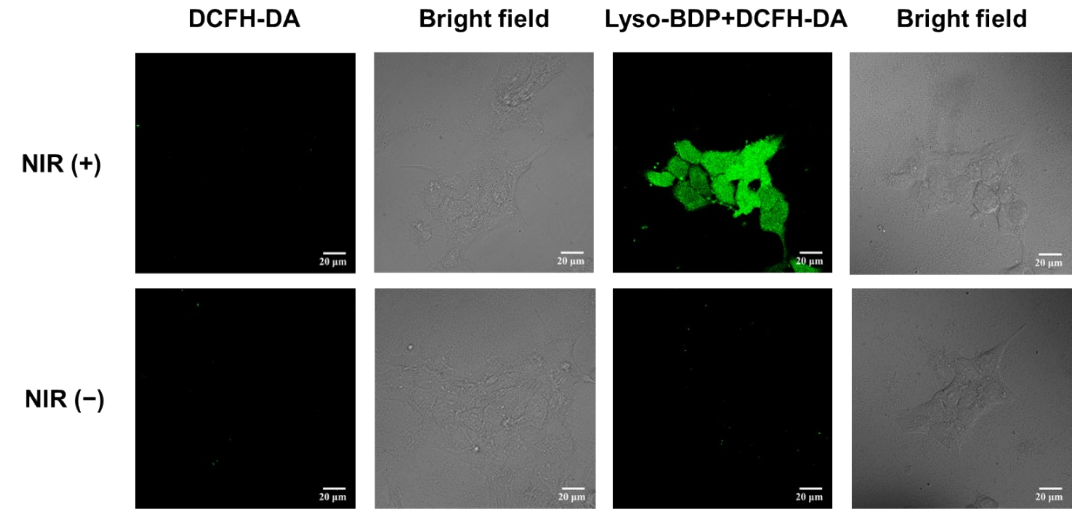

Fig. S16. Confocal fluorescence images of intracellular $^1O_2$ production in 4T1 cells using DCFH-DA assay. Green channel emission was collected at 480-520 nm uponexcitation at 488 nm. Scale bar, 20 μM. (660 nm, 1 W/cm^2, 5 min).

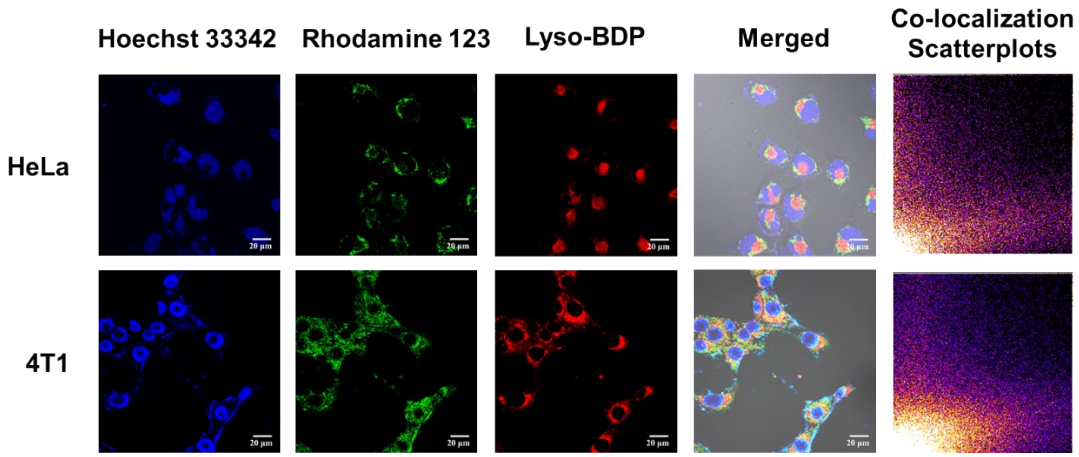

Fig. S17. Subcellular colocalization images with Hoechst 33342, Rhodamine 123 and product staining. The correlation coefficient of product and LysoTracker Green in HeLa cells (A) and in 4T1 cells (B) is 0.065 and 0.120. Ex: 405 nm, Em: 430-470 nm (blue channel); Ex: 488 nm, Em: 540-580 nm (green channel); Ex: 640 nm, Em:700-800 nm (red channel). Scale bars: 20 μm.

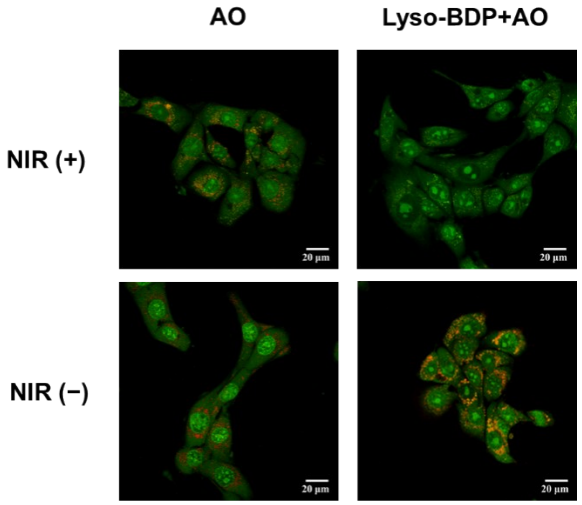

Fig. S18. Confocal fluorescence observation of lysosomal stability of 4T1 cells after different treatments. Ex: 488 nm; Em: 515-545 nm (green channel); 610-640 nm (red channel). Scale bar, 20 μM. (660 nm, 1 W/cm^2, 5 min).

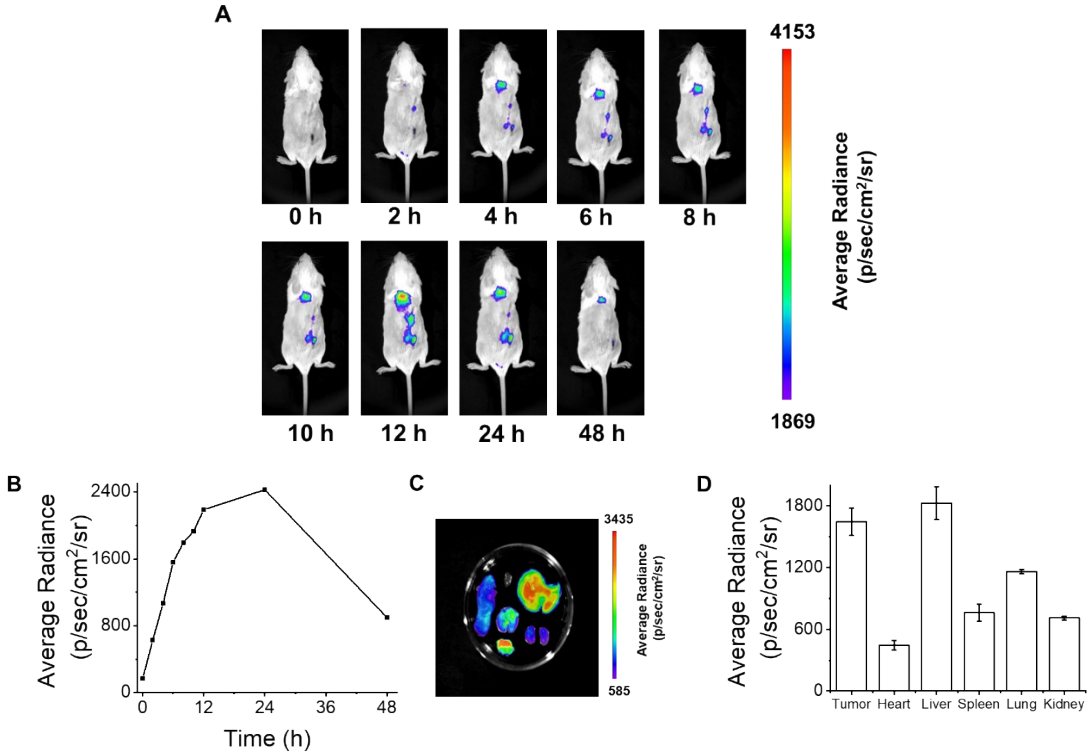

Fig. S19. (A) Real-time fluorescence imaging of tail vein injection of Br-BDP (1 mg/kg) at different times; (B) Real-time fluorescence intensity at different times. (C) Biological distribution of Br-BDP in tumor, heart, liver, spleen, lung and kidney tissues. (D) Mean fluorescence intensity of 4T1 tumor-bearing mice after injection of Br-BDP 24 hours by tail vein.

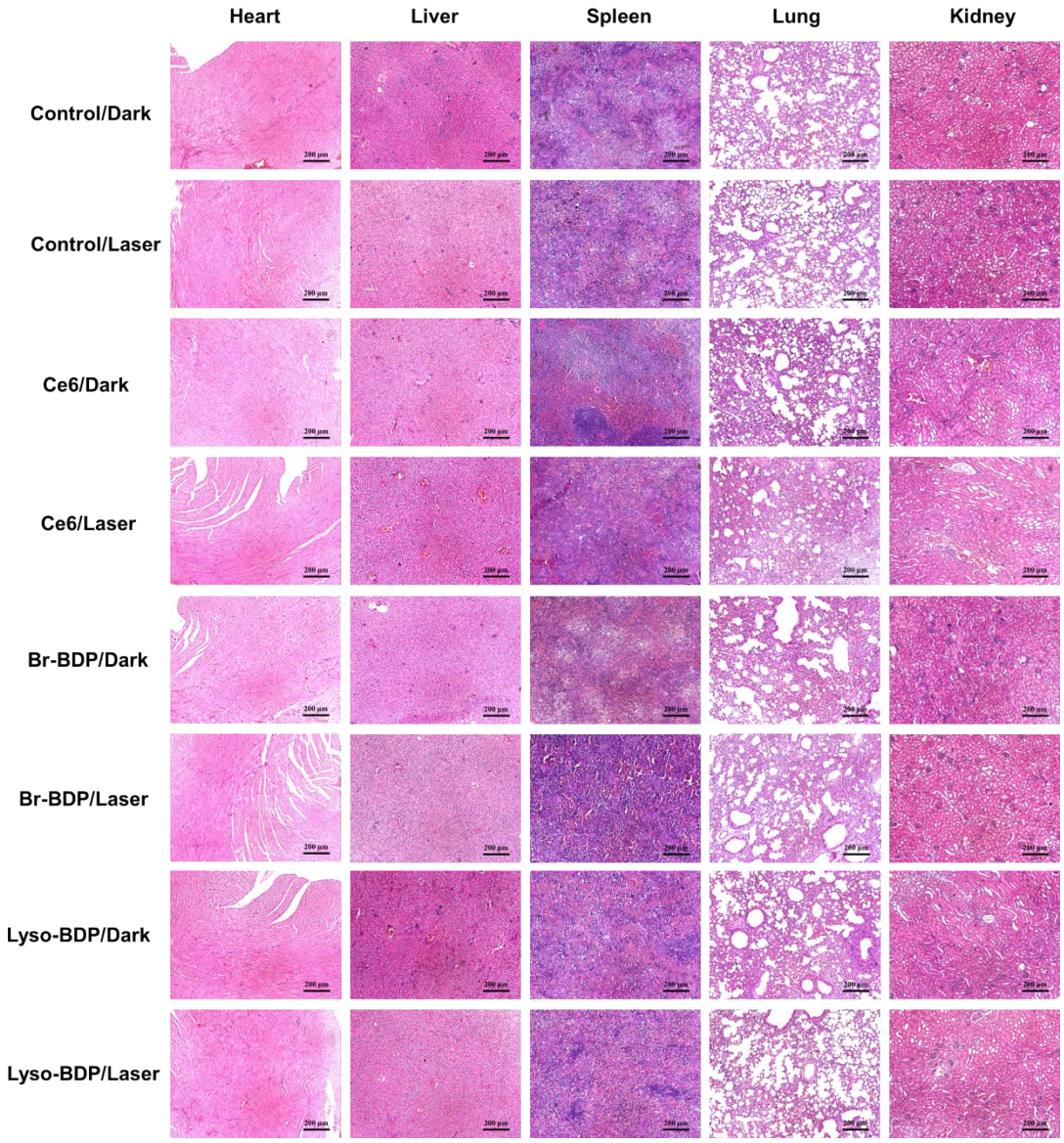

Fig. S20. H&E staining images of main organ tissue sections in tumor bearing mice of different experimental groups. Scale bar, 200 μm.

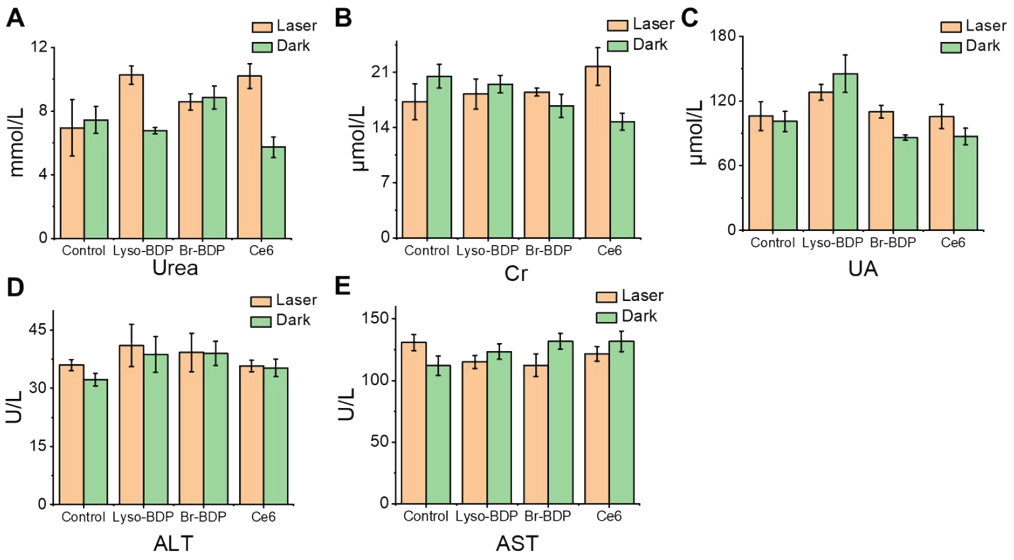

Fig. S21. Hematological parameters of each experimental group after light radiation or in darkroom. (A-C) Renal function markers: urinary creatinine/Ucrea, creatinine/Cr, uric acid /UA, (D, E) Liver function markers: alanine aminotransferase/ALT, aspartate aminotransferase/AST.

Table S1. Photophysical properties of compounds*

Compoud	Solvent	λ_{max} (nm)		Stocks Shifts (nm)	ε (mol^{-1} cm^{-1} L)	Singlet oxygen quantum yield [b]	Fluorescence quantum yield [a]
		Abs	Em				
Lyso-BDP	DMSO	628	725	97	52670	0.0237	/
	MeOH	615	706	91	67330	/	0.1044
	PB (0.3% DMSO)	632	770	138	40000	/	/
Br-BDP	DMSO	636	735	99	66670	0.0192	/
	MeOH	625	712	87	51000	/	0.1136
	PB (0.3% DMSO)	618	755	137	29330	/	/

*[a]: Cresyl violet acetate as a standard and its fluorescence quantum yield in MeOH is 0.55;
[b]: Methylene blue as a reference, the singlet oxygen quantum yield in DMSO is 0.52.

References

[1] H.S. Jung, J.-H. Lee, K. Kim, S. Koo, P. Verwilst, J.L. Sessler, C. Kang, J.S. Kim, A mitochondria-targeted cryptocyanine-based photothermogenic photosensitizer, J. Am. Chem. Soc. 139 (2017) 9972–9978. https://doi.org/10.1021/jacs.7b04263.